

## Investigation of aquifer-system compaction in the Hueco basin, El Paso, Texas, USA

CHARLES HEYWOOD

US Geological Survey, Water Resources Division, 4501 Indian School Road NE, Suite 200, Albuquerque, New Mexico 87110, USA

**Abstract** The Pleistocene geologic history of the Rio Grande valley in the Hueco basin included a cycle of sediment erosion and re-aggradation, resulting in unconformable stratification of sediment of contrasting compressibility and stress history. Since the 1950s large groundwater withdrawals have resulted in significant water-level declines and associated land subsidence. Knowledge of the magnitude and variation of specific storage is needed for developing predictive models of subsidence and groundwater flow simulations. Analyses of piezometric and extensometric data in the form of stress-strain diagrams from a 16 month period yield *in situ* measurements of aquifer-system compressibility across two discrete aquifer intervals. The linear elastic behaviour of the deeper interval indicates over-consolidation of basin deposits, probably resulting from deeper burial depth before the middle Pleistocene. By contrast, the shallow aquifer system displays an inelastic component, suggesting pre-consolidation stress not significantly greater than current effective stress levels for a sequence of late Pleistocene clay. Harmonic analyses of the piezometric response to earth tides in two water-level piezometers provide an independent estimate of specific storage of aquifer sands.

### INTRODUCTION

The Hueco basin is a fault-bounded structural depression associated with the Rio Grande Rift (Fig. 1). From the late-Tertiary to the middle Pleistocene, the basin aggraded with alluvial deposits associated with an ancient fluvial system. In the middle Pleistocene, the modern Rio Grande penetrated the basin and eroded approximately 150 m of early Pleistocene basin fill to form the Rio Grande valley. The river has since deposited approximately 60 m of gravel, sand and clay. This cycle of erosion and deposition has resulted in unconformable stratification of unconsolidated late Pleistocene and Holocene sediment above over-consolidated early Pleistocene alluvium.

The two million inhabitants of El Paso, Texas, and Juarez, Mexico, create a large demand for water in an arid environment. Much of this demand is supplied by groundwater pumpage from the Hueco basin aquifer system underlying El Paso and Juarez, resulting in water table declines of more than 50 m. Precision geodetic measurements indicate land subsidence of as much as 0.3 m since the mid 1950s. Adverse effects have occurred in local areas of shallow differential compaction of late Pleistocene sediments (Land & Armstrong, 1985).

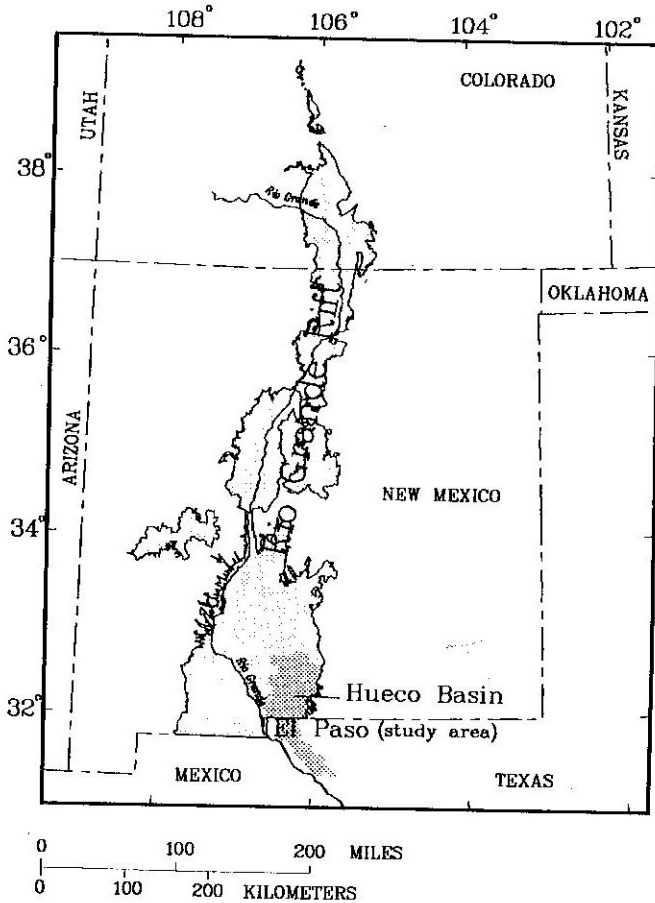


Fig. 1 Map showing location of Rio Grande rift, Hueco Basin and El Paso study area.

## STRAIN AND PRESSURE MEASUREMENT

In order to discriminate the components of vertical deformation due to groundwater production in the deeper early Pleistocene alluvium from those occurring in the Holocene river alluvium, a pair of highly-sensitive vertical extensometers was installed in the aquifer system adjacent to the Rio Grande in 1992. Riley (1986) elucidated the fundamental requirements for precision borehole extensometry, which Heywood (1994) applied to the installation in El Paso (Fig. 2). A shallow-extensometer spans the interval 6-100 m depth, which includes the recent river alluvium (Fig. 3). A deeper extensometer spans the interval 6-340 m, which also includes the interval of production from the regional aquifer system. Bi-hourly displacement measurements made with linear potentiometers have a resolution of several microns. Tests of displacement sensitivity indicated frictional deadband less than 20 microns in either extensometer, corresponding to strain sensitivity less than  $2 \times 10^{-7}$  for the shallow extensometer and  $6 \times 10^{-8}$  for the deep extensometer. A 16 month record of the displacement time series for both extensometers is depicted in Fig. 4(a). (Digital data for September 1993 were lost due

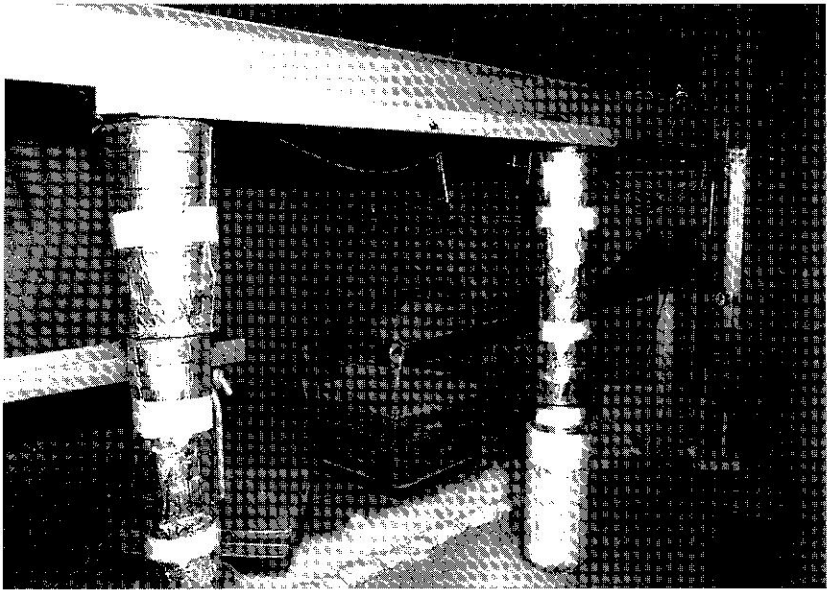


Fig. 2 Photograph of deep extensometer, counter-weight lever arm, and surface datum table.

to failure of data logger electronics.) A key feature of this extensometer installation is the precise reference of both extensometers to the same surface datum, thus the difference between the two extensometer signals measures vertical compaction in the 100-340 m interval of the regional aquifer system. Because the mechanical components of both extensometers are nearly identical at the surface, the small temperature effects in each extensometer are largely cancelled in this signal-difference measurement.

Seven piezometers were installed to measure pore pressure at various depths in the aquifer system. Figure 3 displays a geophysical log of electrical resistivity obtained from the deepest extensometer hole. The depth and thickness of sand (high resistivity) vs. clay (low resistivity) strata may be inferred in the shallow brackish and fresh-water zones to approximately 230 m depth. Increasingly saline water below this depth causes low apparent electrical resistivity of the formation. (TDS of water in the piezometer screened at 320 m depth was  $1 \times 10^4$  mg l<sup>-1</sup>.) Piezometer screens 3 m in length were placed in selected sand intervals, the depths of which are indicated by accented shades in Fig. 3. The inverted solid triangles in Fig. 3 indicate the average piezometric head for each piezometer. A large downward vertical hydraulic gradient exists from the river to the production interval of the regional aquifer system, which is between 100-230 m depth. Water is also occasionally injected into this fresh water interval for storage and to retard vertical diffusion of overlying brackish and underlying saline groundwater. Bi-hourly pressure measurements resolved 20 Pa of pressure or 2 mm of water level change. Maximum amplitudes of pore-pressure change were measured in the piezometer screened at 201-204 m depth, in response to withdrawal from and injection into the regional aquifer system. A 16 month record of piezometric drawdowns at 55-58 and 201-204 m depth is depicted in Fig. 4(b). The similarity in form of the piezometric hydrograph for 201-204 m depth (Fig. 4(b)) with the deep extensometer displacement

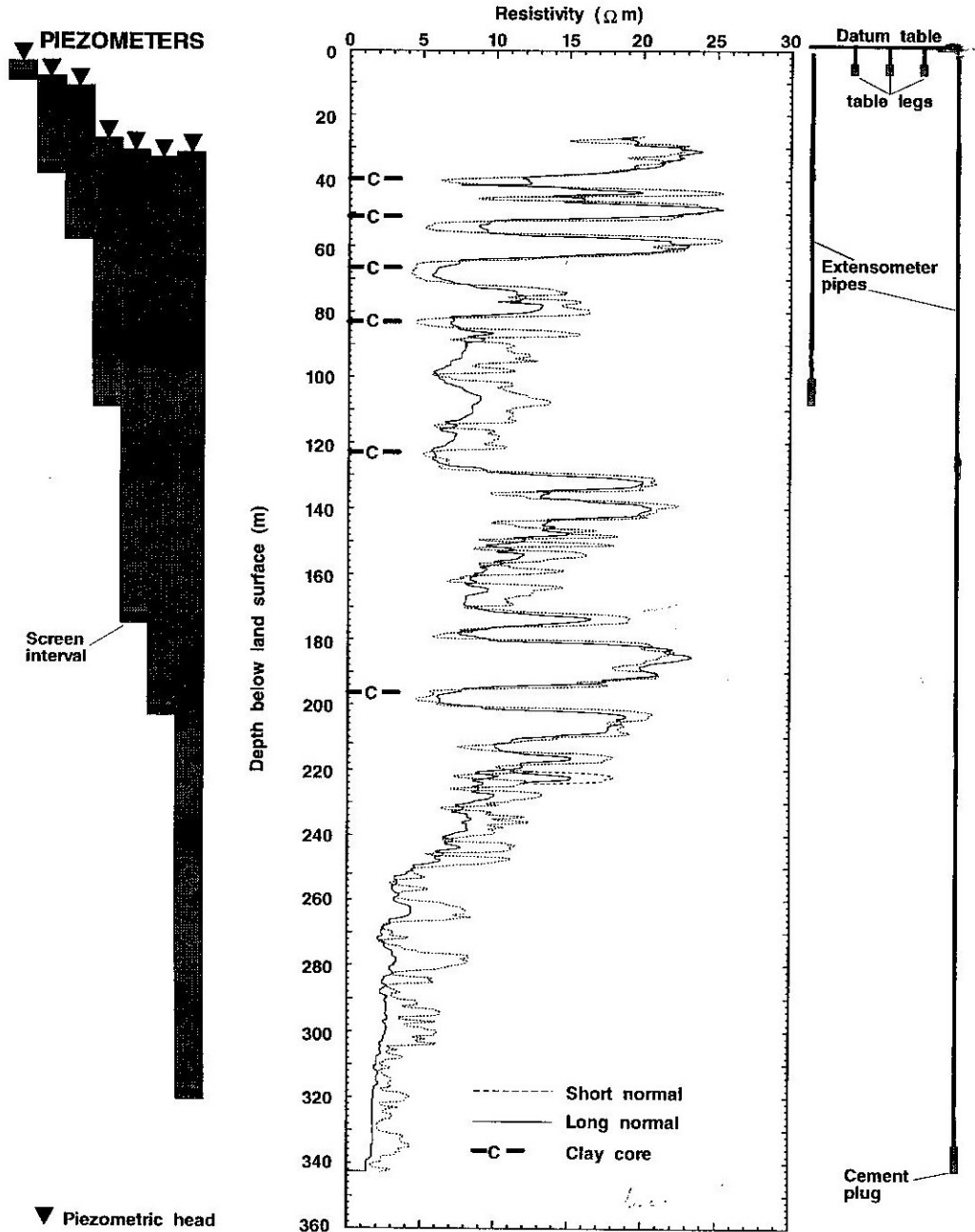


Fig. 3 Resistivity logs with piezometer and extensometer depth intervals (explained in text).

record for the same time period (Fig. 4(a)) indicates that pressure changes in this interval principally effect gross aquifer-system compaction at the extensometer site.

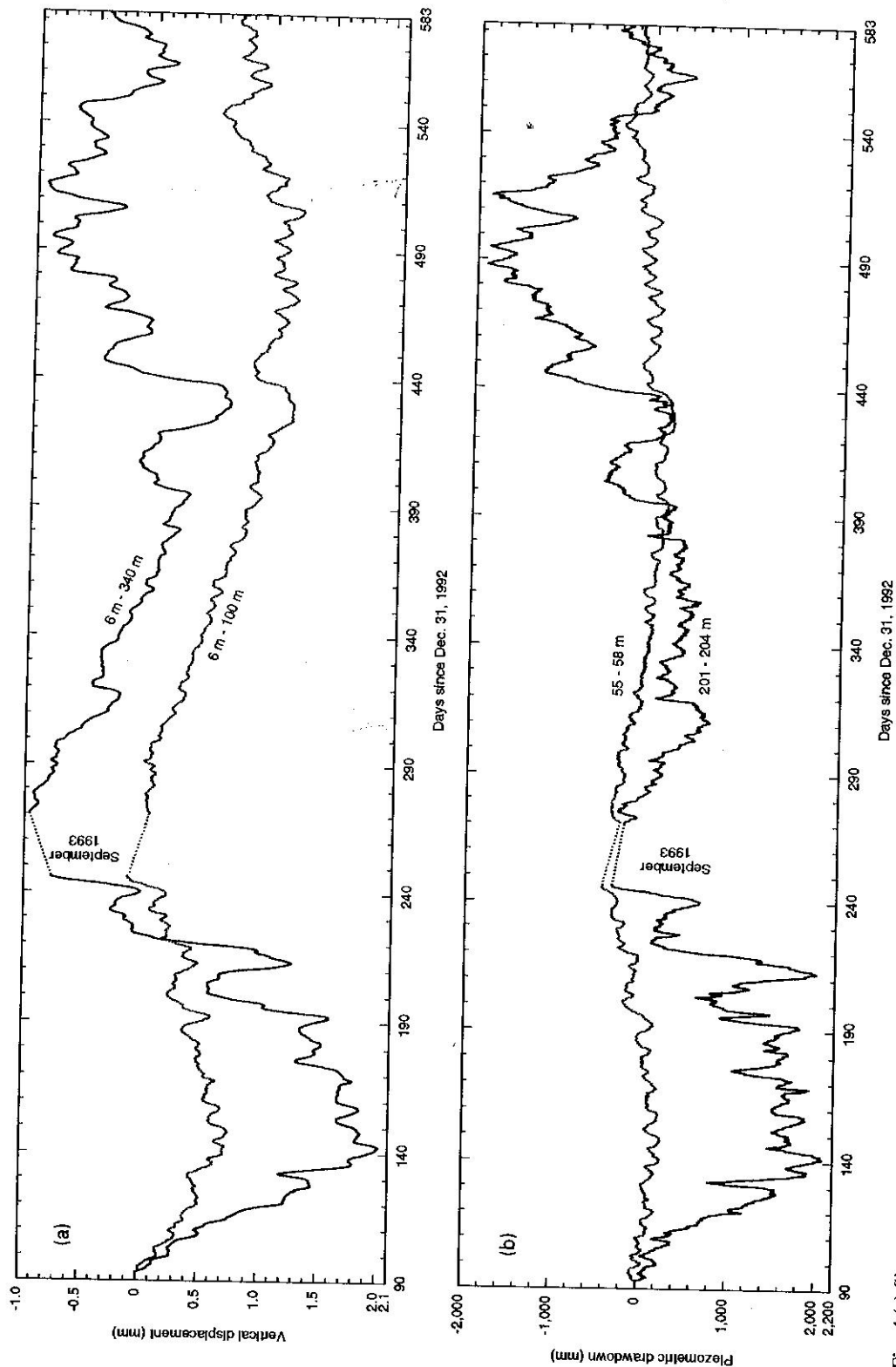


Fig. 4 (a) Sixteen month displacement records from shallow and deep extensometers. (b) Sixteen month hydrographs of piezometers screened at 55-58 and 201-204 m depth.

## DETERMINATION OF AQUIFER-SYSTEM SPECIFIC STORAGE

The specific storage of porous media is given by  $S_s = \rho g (\alpha + n \beta)$ , where  $\rho$  is the density of water,  $g$  is the acceleration of gravity,  $\alpha$  is the vertical compressibility of the granular matrix,  $\beta$  is the compressibility of water, and  $n$  is the porosity. This definition of  $S_s$  includes a skeletal portion  $S_{sk}$  governed by the matrix compressibility, and a portion  $S_{sw}$  due to the compressibility of water contained in the matrix pore space. Solid grains are much stiffer than the alluvial skeletal matrix they comprise, and are considered incompressible. The skeletal portion  $S_{sk}$  may have both elastic  $S_{ske}$  and inelastic  $S_{skv}$  components, the magnitude of which depend on both the magnitude and frequency of the applied stress and the stress history of the compressible materials (Helm, 1976; Galloway, 1994).

### Extensometric-piezometric determination of aquifer-system matrix compressibility

Riley (1970) demonstrated the utility of plots of piezometric head vs. vertical compaction data for determining elastic and inelastic components of aquifer system skeletal specific storage. Vertical strain  $\epsilon_{33}$  for the interval 100-340 m depth was calculated from the difference between the deep and shallow extensometer displacement time series, divided by 240 m (the difference in length between the deep and shallow extensometers). Figure 5(a) is a plot of decrease in pore pressure at 201-204 m depth vs.  $\epsilon_{33}$  for the data depicted in Figs 4(a) and 4(b). Because the water table did not change during the periods of these pressure fluctuations, a unit decrease in pore pressure results in a unit increase in effective stress. The ordinate of Fig. 5(a) is therefore equivalent to increased effective stress in the aquifer matrix at 201-204 m depth. The inverse slope  $2.7 \times 10^{-10} \text{ Pa}^{-1}$  in this plot under-estimates the average matrix compressibility  $\alpha$  for the aquifer system between 100-340 m depth because the distribution of pore pressure variation over this interval is non-uniform and generally smaller in magnitude than that measured at 201-204 m depth. A vertical distribution of pore pressure variation constrained by hydrographs at four depths between 100-340 m depth was assigned according to the distribution of sand and clay inferred from the borehole geophysical logs (Fig. 3). The average pore-pressure variation was approximately 35% of that measured in the piezometer screened from 201-204 m depth, resulting in an adjusted  $\alpha = 7 \times 10^{-10} \text{ Pa}^{-1}$ , corresponding to  $S_{ske} = 7 \times 10^{-6} \text{ m}^{-1}$  for the interval from 100-340 m depth.

Because of negligible frictional deadband in either extensometer, the loops in Fig. 5(a) represent hydrodynamic lag between the change in stress measured in the permeable sand at 201-204 m depth and strain in the less permeable fractions of the aquifer system. The width of these loops is related to the permeability and thickness of aquitards within the aquifer system (Riley, 1970).

Over the 16 month period from 3 April 1993 to 5 August 1994, a net expansive strain of  $4 \times 10^{-6}$  occurred with increased pore pressure of only 2 kPa at 201-204 m depth. This elastic expansion may have resulted from either:

- (a) net lowering of the water table, which decreased the geostatic stress in the deeper aquifer system interval, or
- (b) groundwater injection resulting in greater pore pressure increase in a stratigraphic zone above or below that measured at 201-204 m depth.

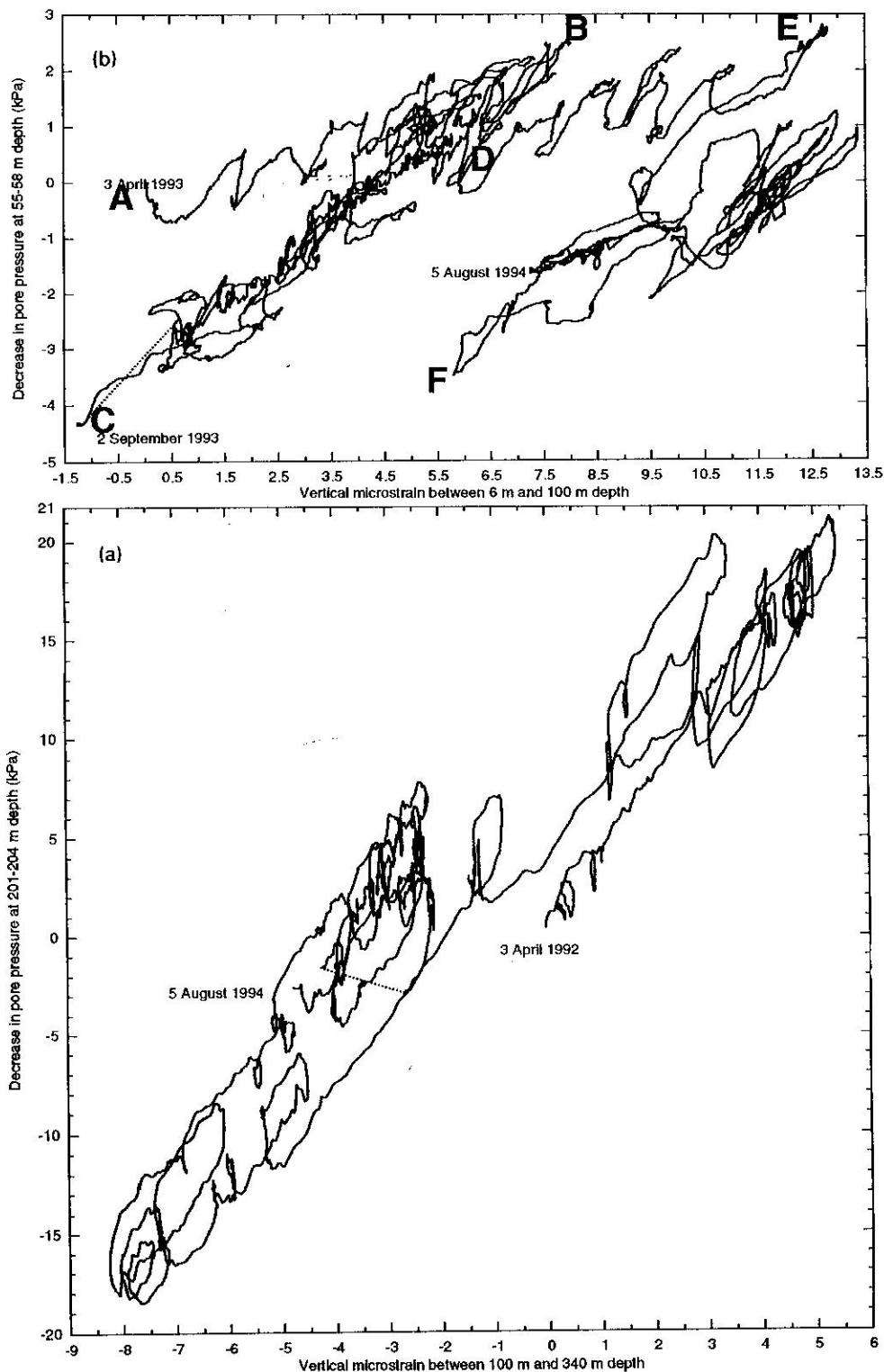


Fig. 5 (a) Stress-strain diagram (explained in text) for aquifer depth interval 100-340 m. (b) Stress-strain diagram (explained in text) for aquifer depth interval 6-100 m.

Two distinct slope trends are apparent in Fig. 5(b), which plots decrease of pore pressure measured in the piezometer screened from 55-58 m depth vs. strain measured by the shallow extensometer between 6 and 100 m depth. The shallow trends of limbs A-B and D-E reflect virgin consolidation of late Pleistocene clays above 60 m. The initial limb A-B of generally declining pore pressure attains a maximum increase in effective stress near point B, which is followed by a second limb B-C of cyclical recovery and drawdown. These two limbs have distinctly different slope, suggesting a stiffer mechanical response along limb B-C at effective stress levels less than the preconsolidation stress attained at point B. Subsequent drawdown increased effective stress levels near that attained at B and resulted in further inelastic consolidation along limb D-E, with preconsolidation stress set slightly higher at the time of point E. Further drawdown and recovery until 5 August 1994 on limb E-F occurred with compressibility similar to limb B-C.

Right leaning cusps between points A and E may represent virgin consolidation of late Pleistocene clays above 60 m depth superimposed upon the stiffer elastic response of coarse interbeds and underlying early Pleistocene sediment. Gently sloping cusp tops result from virgin consolidation and trend parallel to the net displacements from A to B and D to E. Geophysical logs suggest aggregate clay thickness of 20 m above 60 m depth. If inelastic deformation is occurring in this sequence of clays,  $\alpha$  is approximately  $1 \times 10^{-8} \text{ Pa}^{-1}$  for virgin consolidation of late Pleistocene clay, corresponding to  $S_{skv} = 1 \times 10^{-4} \text{ m}^{-1}$ . The steeper cusp flanks with inverse slope  $\alpha = 6 \times 10^{-10} \text{ Pa}^{-1}$  suggest  $S_{ske} = 6 \times 10^{-6} \text{ m}^{-1}$  for the older and coarse sediment fraction in the interval from 6-100 m depth. Limbs B-C and E-F have a slightly shallower slope than the steep cusp flanks, reflecting the somewhat softer elastic response of the entire stratigraphic sequence between 6-100 m compared the coarse fraction. The inverse slope  $\alpha = 1 \times 10^{-9} \text{ Pa}^{-1}$  of these limbs corresponds to  $S_{ske} = 1 \times 10^{-5} \text{ m}^{-1}$ .

### Determination of sand specific storage from piezometric earth-tide response

Piezometers screened from 106-109 and 201-204 m depth responded to solid earth tides. The magnitudes of the measured responses were analyzed to constrain  $S_s$  of aquifer sands at these depths. Piezometric data were resampled at an hourly interval for each well and grouped into equal length time series of 42.67 days. Corresponding time series of theoretical horizontal strain ( $\epsilon_{11} + \epsilon_{22}$ ) due to solid earth tides at the piezometer location were calculated with the algorithm of Harrison (1971). To determine the piezometric response due to each earth-tide harmonic, each time series was filtered with a 7th order Butterworth high-pass filter using a cutoff frequency of 0.7 cycles day<sup>-1</sup> and fit to a sum-of-sines-and-cosines function using least squares:

$$x(t_j) = \sum_{n=1}^N a_k \cos(2\pi\omega_k t_j) + b_k \sin(2\pi\omega_k t_j) + R_j$$

where:  $x(t_j)$  represents the reduced data at time  $t_j$ ,  $t_j$  is the time of data point  $j$ ,  $N = 6$  (the number of tidal harmonics in the analysis),  $\omega_k$  is the frequency of the  $k$ th tidal harmonic (Table 1),  $a_k$  and  $b_k$  are regression coefficients, and  $R_j$  is the residual of data point  $j$  in the reduced record. The amplitude of the piezometric response to a particular

**Table 1** Tidal harmonics used in regression analysis (Bartels, 1957).

Tide	Frequency (day <sup>-1</sup> )	Period (hours)
S2 Principal solar	2.000000000	12.00000000
M2 Principal lunar	1.932273614	12.42060121
N2 Lunar ellipticity	1.895981969	12.65834823
K1 Lunisolar	1.002737909	23.93446961
O1 Lunar declination	0.929535706	25.81934169
Q1 1st order elliptic from O1	0.893244067	26.86835647

**Table 2** Piezometric sensitivities to earth tides and calculated  $S_s$  for M2.

Piezometer screen interval (m)	N	$p(\epsilon_{11} + \epsilon_{22})^{-1}$ for M2 (GPa)		$p(\epsilon_{11} + \epsilon_{22})^{-1}$ for O1 (GPa)		$S_s$ for M2 (m <sup>-1</sup> )
		Mean	Std. error	Mean	Std error	
106-109	5	1.1	0.3	2.2	1.3	5.9 x 10 <sup>-6</sup>
201-204	11	1.4	0.1	1.6	0.8	4.6 x 10 <sup>-6</sup>

harmonic was found from the regression coefficients  $A_k = (a_k^2 + b_k^2)^{1/2}$  and the phase from  $\phi_k = \text{atan}(-b_k/a_k)$  (Cryer, 1986). A similar regression fit determined the amplitude and phase of each tidal harmonic in the theoretical horizontal strain ( $\epsilon_{11} + \epsilon_{22}$ ) associated with each sample time series. The ratios of piezometric responses ( $p$ ) to horizontal strain amplitudes, or horizontal strain sensitivities ( $p(\epsilon_{11} + \epsilon_{22})^{-1}$ ), were calculated for the M2 and O1 frequencies and are summarized in Table 2. Standard errors of horizontal strain sensitivity were larger for O1 than M2 because the amplitude of tidal horizontal strain at the O1 frequency is approximately one half the amplitude at the M2 frequency. By assuming a Poisson ratio = 0.25, specific storage was calculated for the M2 frequency using the relation (Bredehoeft, 1967; Hsieh *et al.*, 1988):

$$S_s = \rho g \frac{1 - 2\nu}{1 - \nu} \frac{(\epsilon_{11} + \epsilon_{22})}{p}$$

Pressure diffusion can attenuate horizontal strain sensitivity, causing magnitudes of specific storage to appear frequency dependent at tidal frequencies. Although the magnitudes of horizontal strain sensitivity for O1 and M2 agree within the range of the standard error for O1, this standard error is relatively large. Therefore, some frequency dependence of  $S_s$  may exist at these tidal frequencies. Drainage effects may also be quantified by examining the frequency dependence of the barometric efficiency (Galloway, 1994; Rojstaczer, 1988). At the piezometer location in El Paso, random pumping stress contaminated the piezometric response to atmospheric loading, causing incoherent frequency response of the barometric efficiency. It was therefore not possible to further quantify the magnitude of possible attenuation of horizontal strain sensitivity.

## COMPARISON OF ELASTIC SPECIFIC STORAGE ESTIMATES

The stress-strain plots provide estimates of  $S_{ske}$  integrated over aquifer system intervals from 6-100 and 100-340 m depth and  $S_{skv}$  for late Pleistocene clay above 60 m depth. If a porosity of 0.3 is assumed and  $\beta = 4.4 \times 10^{-10} \text{ Pa}^{-1}$ ,  $S_{sw} = 1.3 \times 10^{-6} \text{ m}^{-1}$  may be added to these skeletal components to estimate the average  $S_s$  for these intervals, which are summarized in Table 3. The average  $S_s$  measured by extensometric-piezometric analysis decreases between the 6-100 m interval and the 100-340 m interval. This trend is also apparent from the magnitudes of  $S_s$  for sands at 106-109 and 201-204 m depth determined from earth tide analyses, and probably reflects a general trend of smaller matrix compressibilities with larger confining pressures.

**Table 3** Summary of elastic specific storage estimates.

Depth interval (m)	Method	Lithology	$S_{ske}$ ( $\text{m}^{-1}$ )	$S_s$ ( $\text{m}^{-1}$ )
6-100	Extensometric	sands and clays	$1.0 \times 10^{-5}$	$1.1 \times 10^{-5}$
6-100	Extensometric	sands	$6 \times 10^{-6}$	$7.3 \times 10^{-6}$
106-109	Tidal response	sand		$5.9 \times 10^{-6}$
201-204	Tidal response	sand		$4.6 \times 10^{-6}$
100-340	Extensometric	sands and clays	$7 \times 10^{-6}$	$8 \times 10^{-6}$

The magnitudes of  $S_s$  for sands at 106-109 and 201-204 m depth are smaller than the average for the interval 100-340 m depth determined from extensometric-piezometric analysis. This suggests that the clay fraction in this interval has somewhat higher  $S_s$  than the average for the interval as a whole. A similar difference is observed in the upper aquifer-system interval from 6-100 m depth, for which the  $S_s$  inferred for sands is elastically stiffer than the average for sand and clay in the interval. It is noteworthy that  $S_s$  for sands in either interval is approximately  $2.8 \times 10^{-6} \text{ m}^{-1}$  less than the average for sand and clay in the corresponding interval. The larger  $S_s$  determined from extensometric-piezometric analysis may partly result from the lower frequencies of stress changes measured by this method (Galloway, 1994). At the lower frequencies pore pressures within the clays can more nearly approach equilibrium with adjacent sands. As a result, average changes in effective stress are larger and the concomitant changes in strain are greater.

## REFERENCES

- Bartels, J. (1957) Tidal forces. In: *Earth Tides* (ed. by J. C. Harrison), 25-63. Van Nostrand Reinhold Co., New York.
- Bredehoeft, J. D. (1967) Response of well-aquifer systems to earth tides. *J. Geophys. Res.* 72(12), 3075-3087.
- Cryer, J. D. (1986) *Time Series Analysis*. Duxbury Press, Boston, Massachusetts.
- Galloway, D. L. (1994) The frequency dependence of aquifer-system elastic storage coefficients, implications for estimates of aquifer hydraulic properties and aquifer-system compaction. In: *U.S. Geological Survey Subsidence Interest Group Conference* (ed. by K. R. Prince, D. L. Galloway & S. A. Leake) (Edwards Air Force Base, Antelope Valley, California, November 18-19, 1992), Abstracts and Summary. *USGS Open-File Report 94-532*.
- Harrison, D. H. (1971) New computer programs for the calculation of earth tides, Cooperative Institute for Research in Environmental Sciences, NOAA/University of Colorado.

- Helm, D. C. (1976) One-dimensional simulation of aquifer system compaction near Pixley, California. 2. Stress dependent parameters. *Wat. Resour. Res.* 12(3), 375-391.
- Heywood, C. E. (1994) Monitoring aquifer compaction and land subsidence due to groundwater withdrawal in the El Paso, Texas - Juarez, Chihuahua area. In: *U.S. Geological Survey Subsidence Interest Group Conference* (ed. by K. R. Prince, D. L. Galloway & S. A. Leake) (Edwards Air Force Base, Antelope Valley, California, November 18-19, 1992), Abstracts and Summary. *USGS Open-File Report 94-532*.
- Hsieh, P. A., Bredehoeft, J. D. & Rojstaczer, S. A. (1988) Response of well aquifer systems to earth tides: problem revisited. *Wat. Resour. Res.* 24(3), 468-472.
- Land, L. F. & Armstrong, C. A. (1985) A preliminary assessment of land-surface subsidence in the El Paso area, Texas. *USGS Water-Resources Investigations Report 85-4155*.
- Riley, F. S. (1970) Analysis of borehole extensometer data from central California. In: *Land Subsidence* (Proc. Tokyo Symp., 1969), vol. 2, 423-431. IAHS Publ. no. 89.
- Riley, F. S. (1986) Developments in borehole extensometry. In: *Land Subsidence* (ed. by A. I. Johnson, L. Carbognin & L. Ubertini) (Proc. Venice Symp., March 1984), 169-186. IAHS Publ. no. 151.
- Rojstaczer, S. A. (1988) Determination of fluid flow properties from the response of water wells to atmospheric loading. *Wat. Resour. Res.* 24, 1927-1938.